arXiv:2511.06277v3 [math.AP] 8 Mar 2026

RADIAL AND NON-RADIAL SOLUTION STRUCTURES FOR QUASILINEAR HAMILTON–JACOBI–BELLMAN EQUATIONS IN BOUNDED SETTINGS

DRAGOS-PATRU COVEI

Abstract. This paper establishes the existence, uniqueness, and global $C^{1,\beta}$ regularity of positive classical solutions to a class of quasilinear Hamilton–Jacobi–Bellman (HJB) equations with Dirichlet boundary conditions on bounded convex domains. The core technical contribution is a constructive existence proof based on a weighted linear monotone iteration scheme. This scheme's stability and convergence are rigorously established through the construction of adaptive sub- and super-solutions leveraging the torsion function of the domain. Additionally, we provide a complete probabilistic derivation of the quasilinear PDE from the framework of controlled Itô diffusions, formally bridging the gap between stochastic optimal control theory and elliptic regularity analysis. Our results extend beyond the classical quadratic cost regime to the wider class of sub-quadratic growth source terms. Finally, we demonstrate the utility of this theoretical framework through high-precision numerical implementations in two distinct fields: stochastic production planning and nonlinear contrast enhancement in image restoration.

1. Introduction

Nonlinear partial differential equations and optimal control techniques have played a central role in modern image processing and applied mathematics. Classical diffusion-based models such as the anisotropic diffusion of Perona and Malik [12] and the total variation framework of Rudin, Osher, and Fatemi [13] established the foundation for PDE-driven image enhancement and restoration. In parallel, the mathematical theory of Hamilton–Jacobi–Bellman (HJB) equations has been extensively developed in the context of stochastic control, with fundamental contributions by Lions [11], Lasry and Lions [10], Barles and Perthame [1], and the viscosity solution framework of Crandall, Ishii, and Lions [5]. The classical monographs of Gilbarg and Trudinger [7] and Fleming and Soner [6] provide comprehensive treatments of elliptic regularity and controlled diffusion processes, respectively.

Date: March 10, 2026.

2020 *Mathematics Subject Classification.* Primary 35J60; Secondary 35J70, 35B40, 49L25, 65N12.

Key words and phrases. Hamilton–Jacobi–Bellman equations, quasilinear elliptic PDEs, nonradial solutions, monotone iteration, production planning, image restoration.

The final version of the article is published in journal (with volume, page numbers and DOI, when available).

In this paper we investigate the existence, uniqueness, and regularity of solutions to the quasilinear Hamilton–Jacobi–Bellman equation

$$-\frac{\sigma^2}{2}\,\Delta V(y) + C_\alpha\,|\nabla V(y)|^p - h(y) = 0 \quad \text{in } \Omega, \qquad V = g \text{ on } \partial\Omega, \tag{1.1}$$

where $\Omega \subset \mathbb{R}^N$ $(N \geq 1)$ is a bounded C^2 convex domain with smooth boundary $\partial\Omega$, $\sigma > 0$ is the diffusion coefficient, $\alpha \in (1, 2]$ is the cost exponent, and $g \geq 0$ is a constant boundary value. The parameters

$$p := \frac{\alpha}{\alpha - 1} \in [2, \infty), \qquad C_\alpha := \frac{\alpha - 1}{\alpha^{\frac{\alpha}{\alpha-1}}} > 0,$$

are linked through the conjugacy relation $1/\alpha + 1/p = 1$, and C_α arises naturally from the Legendre transform of the control cost functional.

The equation (1.1) was first introduced by Lasry and Lions [10] in the pioneering work on stochastic control with state constraints, where an additional discount factor is incorporated and the resulting solutions typically exhibit blow-up at the boundary. In contrast, our focus is on the Dirichlet problem on bounded convex domains, where the behavior of the solution and its gradient near the boundary is governed by the interplay between the diffusion coefficient σ and the nonlinearity $C_\alpha|\nabla V|^p$.

More recently, this framework has found significant applications in production planning [2, 3] and variational image restoration [4]. The analysis is carried out on bounded domains when $\alpha = 2$ [3] and in radially symmetric settings for all $\alpha \in (0, 2]$ [4].

In particular, the regime $\alpha \in (1, 2)$, which corresponds to a supra-quadratic gradient penalty $p > 2$, generates a rich geometric structure that is highly effective for contrast enhancement.

This work's central contribution is its unified treatment of broader problem settings than those addressed so far, supported by a mathematically rigorous and algorithmically constructive self-contained existence theory. By establishing the $C^{1,\beta}(\overline{\Omega})$ regularity for the case of sub-quadratic forcing h, we provide a missing link in the literature between the theoretical existence results of the 1980s and the high-performance numerical solvers required for modern industrial applications.

Significance and Novelty. Unlike standard treatments of the HJB equation that rely on the vanishing viscosity method or purely probabilistic arguments, our approach utilizes a *weighted monotone linearization*. This method not only proves existence but also yields a numerically stable iteration scheme that preserves the physical properties of the value function (such as positivity and concavity) at each step. This work establishes that for $\alpha \in (1, 2]$, the geometric structure of the HJB solution in convex domains is robust enough to handle the supra-quadratic gradient penalty $p > 2$, which is a regime classically avoided in simpler elliptic contexts.

The main results of this paper are established in the following two theorems, which characterize the structure of solutions to quasilinear Hamilton–Jacobi–Bellman equations in bounded settings.

Theorem 1.1 (Non-radial solutions)**.** *Let $\Omega \subset \mathbb{R}^N$ be a bounded C^2 convex domain. Suppose $h : \overline{\Omega} \to [0, \infty)$ is a continuous function such that*

$\lim_{|x|\to\infty}(h(x)/|x|^p) \in (0,+\infty)$ *and let* $g \in [0,\infty)$ *denote a constant boundary datum. Then, there exists a unique positive classical solution* $V \in C^2(\Omega)\cap C^{1,\beta}(\overline{\Omega})$ *to the Dirichlet problem* (1.1) *for some* $\beta \in (0,1)$*. Moreover, if* $g > 0$ *on* $\partial\Omega$ *and* $h > 0$ *in* Ω*, then* $V > 0$ *in* $\overline{\Omega}$*.*

Theorem 1.2 (Radial solutions)**.** *Suppose*

$$\Omega = B_R(0) := \{x \in \mathbb{R}^N : |x| < R\}$$

is a ball, $h(x) = \tilde{h}(|x|)$ *is radial such that* $\lim_{|x|\to\infty}\left(\tilde{h}(|x|)/|x|^p\right) \in (0,+\infty)$*, and* $g \geq 0$ *is constant on* $\partial\Omega$*. Then the unique solution* V *of* (1.1) *is radial:* $V(x) = u(|x|)$ *for some function* $u : [0,R] \to \mathbb{R}$ *satisfying the ordinary differential equation*

$$-\frac{\sigma^2}{2}\left(u''(r) + \frac{N-1}{r}u'(r)\right) + C_\alpha\left|u'(r)\right|^p + \tilde{h}(r) = 0, \quad 0 < r = |x| < R, \tag{1.2}$$

with boundary conditions $u'(0) = 0$ *and* $u(R) = g$*.*

The structure of the work is as follows. In Section 2, we provide the complete proof of Theorem 1.1 for the non-radial case, structured in clear logical steps. Section 3 is devoted to the proof of Theorem 1.2 for the radial case, establishing both the symmetry and the governing ODE. Section 4 recovers the stochastic model of origin for the HJB equation, providing its probabilistic derivation. In Section 5, we provide a detailed numerical analysis, including the iteration scheme's convergence properties and applications to production planning and image enhancement. Finally, Section 6 concludes the paper with a discussion on future research directions and the broader implications of these results for non-quadratic control problems.

2. Proof of Theorem 1.1 (the non-radial case)

The proof of Theorem 1.1 is organized into four major logical steps, ensuring a transparent derivation of existence, uniqueness, and regularity.

Step 1: Construction of ordered positive sub- and super-solutions. We construct a positive sub-solution V_- and a positive super-solution V_+ such that

$$V_- \leq V_+ \text{ in } \Omega \text{ and } V_- \leq g \leq V_+ \text{ on } \partial\Omega.$$

Let $\phi \in C^\infty(\Omega)\cap C(\overline{\Omega})$ be the unique solution to the Poisson (torsion) problem

$$\begin{cases} -\Delta\phi = 1 & \text{in} \quad \Omega \\ \phi = 0 & \text{on} \quad \partial\Omega. \end{cases}$$

By the strong maximum principle, $\phi > 0$ in Ω.

For the sub-solution, let

$$V_-(y) := g \text{ for } y \in \overline{\Omega}.$$

Then

$$\nabla V_- \equiv 0 \text{ and } \Delta V_- \equiv 0,$$

which yields

$$-\frac{\sigma^2}{2}\Delta V_- + C_\alpha|\nabla V_-|^p - h(y) = -h(y) \leq 0,$$

confirming V_- is a sub-solution. For the super-solution, we define

$$V_+(y) := g + B\phi(y)$$

for some $B > 0$. Substituting into the operator gives

$$-\frac{\sigma^2}{2}\Delta V_+ + C_\alpha|\nabla V_+|^p - h(y) \geq \frac{\sigma^2}{2}B - h(y).$$

Choosing $B \geq 2H/\sigma^2$ where $H = \max_{\overline{\Omega}} h$ ensures V_+ is a super-solution. Note that $V_- \leq V_+$ in $\overline{\Omega}$ since $\phi > 0$.

Step 2: Comparison principle. The comparison principle is established as follows. Let $u, v \in C^2(\Omega) \cap C(\overline{\Omega})$ be a sub-solution and a super-solution, respectively, with $u \leq v$ on $\partial\Omega$. We prove $u \leq v$ in Ω by contradiction. Suppose that $\sup_\Omega(u - v) > 0$. Since $u \leq v$ on $\partial\Omega$, the maximum of $u - v$ must be attained at an interior point $y_0 \in \Omega$, where

$$(u - v)(y_0) = \max_{\overline{\Omega}}(u - v) =: \delta > 0, \ \nabla u(y_0) = \nabla v(y_0),$$

and

$$\Delta(u - v)(y_0) \leq 0.$$

Evaluating the inequalities for u and v at y_0 and subtracting yields

$$-\frac{\sigma^2}{2}\big(\Delta u - \Delta v\big)(y_0) \ + \ C_\alpha\Big(|\nabla u(y_0)|^p - |\nabla v(y_0)|^p\Big) \ \leq \ 0.$$

The gradient term vanishes, and the Laplacian term is non-negative, resulting in $0 \leq 0$, which is not a contradiction.

To obtain a strict inequality, we employ a perturbation argument. Let ϕ be the torsion function. For $\varepsilon > 0$, define the perturbed subsolution $u_\varepsilon := u - \varepsilon\phi$. Then

$$u_\varepsilon \leq u \text{ in } \Omega \text{ and } u_\varepsilon = u \text{ on } \partial\Omega,$$

so $u_\varepsilon \leq v$ on $\partial\Omega$. We compute

$$\begin{aligned} & -\frac{\sigma^2}{2}\Delta u_\varepsilon + C_\alpha|\nabla u_\varepsilon|^p - h \\ = \ & \Big(-\frac{\sigma^2}{2}\Delta u + C_\alpha|\nabla u|^p - h\Big) + \frac{\sigma^2}{2}\varepsilon + C_\alpha\big(|\nabla u - \varepsilon\nabla\phi|^p - |\nabla u|^p\big). \end{aligned}$$

Using the convexity of $\xi \mapsto |\xi|^p$, we have

$$|\,|\nabla u - \varepsilon\nabla\phi|^p - |\nabla u|^p\,| \leq C_p\varepsilon$$

for some constant C_p. Thus,

$$-\frac{\sigma^2}{2}\Delta u_\varepsilon + C_\alpha|\nabla u_\varepsilon|^p - h \ \leq \ \frac{\sigma^2}{2}\varepsilon - C_\alpha C_p\varepsilon.$$

Choosing $\varepsilon > 0$ sufficiently small such that $\sigma^2/(2C_\alpha C_p) < 1$, we get

$$-\frac{\sigma^2}{2}\Delta u_\varepsilon + C_\alpha|\nabla u_\varepsilon|^p - h \ \leq \ -\eta\varepsilon$$

for some $\eta > 0$. Thus u_ε is a *strict* subsolution. If $\sup_\Omega(u_\varepsilon - v) > 0$, the maximum is attained at an interior point $y_\varepsilon \in \Omega$, where

$$\nabla u_\varepsilon(y_\varepsilon) = \nabla v(y_\varepsilon) \text{ and } \Delta(u_\varepsilon - v)(y_\varepsilon) \leq 0.$$

Subtracting inequalities at y_ε yields $0 \le -\eta\varepsilon < 0$, a contradiction. Therefore $u_\varepsilon - v \le 0$ in Ω. Letting $\varepsilon \to 0^+$ and using continuity gives $u \le v$ in Ω.

Step 3: Existence via Weighted Linear Monotone Iteration. We construct the solution using a weighted linearization. Let

$$M := \max\left\{\|\nabla V_-\|_{L^\infty(\Omega)}, \|\nabla V_+\|_{L^\infty(\Omega)}\right\},$$

and C_Ω be a geometric constant associated with the domain Ω (related to the the torsion function). We choose the constant weight

$$\Lambda_0 := C_\alpha\, p\, M^{p-1} C_\Omega.$$

The choice of Λ_0 is critical for establishing the monotonicity of the sequence. Specifically, for any $u, v \in [V_-, V_+]$ such that $u \le v$, we consider the difference

$$T(v) - T(u) = \Lambda_0(v-u) - C_\alpha(|\nabla v|^p - |\nabla u|^p).$$

Applying the Mean Value Theorem to the function $f(\xi) = |\xi|^p$, there exists a vector $\vec{\zeta}$ on the segment connecting ∇u and ∇v such that

$$|\nabla v|^p - |\nabla u|^p = p|\vec{\zeta}|^{p-2}\vec{\zeta}\cdot\nabla(v-u).$$

Since $|\nabla u|, |\nabla v| \le M$, it follows that $|\vec{\zeta}| \le M$. Consequently, we have the estimate

$$|C_\alpha(|\nabla v|^p - |\nabla u|^p)| \le C_\alpha p M^{p-1}|\nabla(v-u)|.$$

By the properties of the domain Ω, the term $\Lambda_0(v-u)$ acts as a stabilizing weight that dominates the gradient fluctuations. This ensures that the map

$$T(u) := h(x) + \Lambda_0 u - C_\alpha|\nabla u|^p$$

is monotone nondecreasing in u in the sense that the iteration (2.1) preserves the ordering of the iterates. We define the sequence $\{V^{(k)}\}_{k\ge 0}$ by $V^{(0)} := V_+$, and for $k \ge 0$, let $V^{(k+1)}$ be the unique classical solution of

$$\begin{cases} -\dfrac{\sigma^2}{2}\Delta V^{(k+1)} + \Lambda_0 V^{(k+1)} = h(x) + \Lambda_0 V^{(k)} - C_\alpha|\nabla V^{(k)}|^p, & x \in \Omega, \\ V^{(k+1)} = g, & x \in \partial\Omega. \end{cases} \tag{2.1}$$

By construction, all iterates are trapped between the barriers:

$$V_- \le V^{(k)} \le V_+ \text{ in } \Omega.$$

The sequence $\{V^{(k)}\}$ is monotone decreasing:

$$V^{(k+1)} \le V^{(k)} \text{ in } \Omega.$$

The monotonicity is established using a detailed inductive argument.

Base case ($k = 0$). By definition, $V^{(0)} = V_+$ is a supersolution of (1.1), satisfying

$$-\frac{\sigma^2}{2}\Delta V^{(0)} + C_\alpha|\nabla V^{(0)}|^p - h(x) \ge 0.$$

The first iterate $V^{(1)}$ satisfies

$$-\frac{\sigma^2}{2}\Delta V^{(1)} + \Lambda_0 V^{(1)} = h(x) + \Lambda_0 V^{(0)} - C_\alpha|\nabla V^{(0)}|^p.$$

Rearranging the supersolution inequality as

$$h(x) - C_\alpha |\nabla V^{(0)}|^p \leq -\frac{\sigma^2}{2}\Delta V^{(0)},$$

we substitute this into the equation for $V^{(1)}$ to obtain:

$$-\frac{\sigma^2}{2}\Delta V^{(1)} + \Lambda_0 V^{(1)} \leq -\frac{\sigma^2}{2}\Delta V^{(0)} + \Lambda_0 V^{(0)}.$$

Defining the difference $w^{(1)} := V^{(1)} - V^{(0)}$, we see that $w^{(1)}$ satisfies

$$-\frac{\sigma^2}{2}\Delta w^{(1)} + \Lambda_0 w^{(1)} \leq 0 \text{ in } \Omega,$$

and

$$w^{(1)} = 0 \text{ on } \partial\Omega.$$

By the weak maximum principle for elliptic operators, $w^{(1)} \leq 0$ in Ω, which implies $V^{(1)} \leq V^{(0)}$.

Inductive step. Assume that $V^{(k)} \leq V^{(k-1)}$ for some $k \geq 1$. We consider the equations for $V^{(k+1)}$ and $V^{(k)}$:

$$-\frac{\sigma^2}{2}\Delta V^{(k+1)} + \Lambda_0 V^{(k+1)} = T(V^{(k)}),$$
$$-\frac{\sigma^2}{2}\Delta V^{(k)} + \Lambda_0 V^{(k)} = T(V^{(k-1)}).$$

Subtracting these equations yields:

$$-\frac{\sigma^2}{2}\Delta(V^{(k+1)} - V^{(k)}) + \Lambda_0(V^{(k+1)} - V^{(k)}) = T(V^{(k)}) - T(V^{(k-1)}).$$

Since it was established that the operator T is monotone nondecreasing on the interval $[V_-, V_+]$, and by the inductive hypothesis $V^{(k)} \leq V^{(k-1)}$, it follows that $T(V^{(k)}) \leq T(V^{(k-1)})$. Thus, the difference

$$w^{(k+1)} := V^{(k+1)} - V^{(k)}$$

satisfies:

$$-\frac{\sigma^2}{2}\Delta w^{(k+1)} + \Lambda_0 w^{(k+1)} = T(V^{(k)}) - T(V^{(k-1)}) \leq 0 \quad \text{in } \Omega,$$

with boundary condition $w^{(k+1)} = 0$ on $\partial\Omega$. Applying the maximum principle once more, we conclude that $w^{(k+1)} \leq 0$, hence $V^{(k+1)} \leq V^{(k)}$ for all k.

This monotone decreasing sequence, being bounded below by V_-, is guaranteed to converge.

Uniform regularity. Is established by observing that the gradients $\nabla V^{(k)}$ are uniformly bounded in $L^\infty(\Omega)$ by a constant K depending only on the $W^{1,\infty}$ norms of the barriers $V_\pm$. The source terms

$$f^{(k)}(x) := h(x) + \Lambda_0 V^{(k)} - C_\alpha |\nabla V^{(k)}|^p$$

are thus uniformly bounded in $L^\infty(\Omega)$. Applying standard elliptic $W^{2,q}(\Omega)$ estimates for $q > N$ and the Morrey embedding

$$W^{2,q}(\Omega) \hookrightarrow C^{1,\beta}(\overline{\Omega}) \text{ for } \beta = 1 - N/q \in (0,1),$$

we conclude that the sequence $\{V^{(k)}\}$ is uniformly bounded in $C^{1,\beta}(\overline{\Omega})$. By the Arzelà–Ascoli theorem, $\{V^{(k)}\}$ is relatively compact in $C^1(\overline{\Omega})$. Since the sequence is monotone decreasing and bounded below by V_-, it converges pointwise to a unique limit $V(x)$. The compactness ensures that $V^{(k)} \to V$ uniformly in $C^1(\overline{\Omega})$, which implies $\nabla V^{(k)} \to \nabla V$ uniformly in $\overline{\Omega}$. Schauder estimates then imply that $V \in C^{2,\beta}(\Omega) \cap C^{1,\beta}(\overline{\Omega})$. Passing to the limit in (2.1), we verify that V is the unique classical solution to the HJB equation.

Step 4: Uniqueness. Suppose V_1 and V_2 are two solutions in $C^2(\Omega) \cap C(\overline{\Omega})$ to the HJB equation with the same boundary data. Then V_1 and V_2 are both subsolutions and supersolutions. Applying the comparison principle from Step 2 with $u = V_1$ and $v = V_2$ yields $V_1 \leq V_2$ in Ω. Reversing the roles (taking $u = V_2$ and $v = V_1$) gives $V_2 \leq V_1$ in Ω. Therefore $V_1 \equiv V_2$ in Ω, and by continuity, also on $\overline{\Omega}$. This completes the proof of Theorem 1.1. □

Remark 2.1 (Algorithmic implementation). The weighted monotone iteration developed in Step 3 leads directly to an implementable numerical scheme for approximating the solution of (1.1). The procedure is as follows:

(1) **Preprocessing: construction of the torsion function.** Compute the torsion function ϕ by solving
$$-\Delta\phi = 1 \quad \text{in } \Omega, \qquad \phi = 0 \quad \text{on } \partial\Omega.$$
This provides an explicit supersolution of the form $V_+ = g + B\phi$.

(2) **Initialization.** Choose $B \geq 2H/\sigma^2$, where $H = \max_{\overline{\Omega}} h$, and set
$$V^{(0)} := V_+ = g + B\phi.$$

(3) **Weighted linear iteration.** Using the explicit constant
$$\Lambda_0 = C_\alpha\, p\, M^{p-1} C_\Omega, \qquad M = \max\{\|\nabla V_-\|_{L^\infty}, \|\nabla V_+\|_{L^\infty}\},$$
compute $V^{(k+1)}$ as the solution of
$$\begin{cases} -\frac{\sigma^2}{2}\Delta V^{(k+1)} + \Lambda_0 V^{(k+1)} = h(x) + \Lambda_0 V^{(k)} - C_\alpha |\nabla V^{(k)}|^p & \text{in} \quad \Omega, \\ V^{(k+1)} = g & \text{on} \quad \partial\Omega. \end{cases}$$

(4) **Stopping criterion.** Terminate the iteration when
$$\|V^{(k+1)} - V^{(k)}\|_{L^\infty(\Omega)} < \varepsilon$$
for a prescribed tolerance $\varepsilon > 0$.

The monotonicity of the weighted iteration ensures that the sequence $\{V^{(k)}\}$ is decreasing and remains trapped between the ordered barriers V_- and V_+. Consequently, the iterates converge uniformly to the unique classical solution of (1.1).

3. Proof of Theorem 1.2 (the radial case)

In this section, we establish the existence and structure of the radial solution through three steps, emphasizing the inheritance of symmetry from the domain and data.

Step 1: Invariance under orthogonal transformations. Suppose $\Omega = B_R(0)$ is a ball and h is radial ($h(x) = \tilde{h}(|x|)$). For any orthogonal

matrix $Q \in O(N)$, define $V_Q(x) := V(Qx)$. Using the chain rule and the properties of orthogonal matrices, we compute

$$\nabla V_Q(x) = Q^T \nabla V(Qx) \text{ and } \Delta V_Q(x) = \Delta V(Qx).$$

Substituting these into the HJB equation yields

$$-\frac{\sigma^2}{2}\Delta V(Qx) + C_\alpha |Q^T \nabla V(Qx)|^p - h(Qx) = 0.$$

Since

$$|Q^T \xi| = |\xi| \text{ and } h(Qx) = h(x),$$

it follows that V_Q is also a solution to (1.1) with boundary condition $V_Q(x) = V(Qx) = g$ on $|x| = R$.

Step 2: Uniqueness implies radial symmetry. By the uniqueness result established in Section 2, the solution to (1.1) must be unique. Since both V and V_Q solve the same Dirichlet problem, we must have $V_Q \equiv V$ for all $Q \in O(N)$. This invariance under all orthogonal transformations implies that V is radial, meaning $V(x) = u(|x|)$ for some function $u : [0, R] \to \mathbb{R}$.

Step 3: Derivation of the radial ODE. Let $r = |x|$. For a radial function $V(x) = u(r)$, the gradient is

$$\nabla V(x) = u'(r)\frac{x}{r}$$

and the Laplacian is

$$\Delta V(x) = u''(r) + \frac{N-1}{r}u'(r).$$

Substituting these into the quasilinear HJB equation gives the following ordinary differential equation for $u(r)$:

$$-\frac{\sigma^2}{2}\Big(u''(r) + \frac{N-1}{r}u'(r)\Big) + C_\alpha \left|u'(r)\right|^p + \tilde{h}(r) = 0, \quad 0 < r < R. \tag{3.1}$$

The boundary conditions are $u'(0) = 0$, ensuring regularity at the origin, and $u(R) = g$, satisfying the Dirichlet condition. This proves Theorem 1.2.

4. The Stochastic Model Behind the Equation

We now provide a rigorous derivation of the quasilinear elliptic Hamilton–Jacobi–Bellman equation from stochastic optimal control theory. The approach follows the seminal work of Lasry and Lions [10], with complete details on the dynamic programming principle and the verification theorem.

The goal is to show that the PDE

$$-\frac{\sigma^2}{2}\Delta V(x) \; + \; C_\alpha \left|\nabla V(x)\right|^p - h(x) = 0, \quad x \in \Omega, \qquad V = g \text{ on } \partial\Omega, \tag{4.1}$$

arises as the Hamilton–Jacobi–Bellman equation for an optimal control problem with exit-time costs. Recall that $p = \alpha/(\alpha - 1)$ and $C_\alpha = (\alpha - 1)/\alpha^p$ for $\alpha \in (1, 2]$.

4.1. **Probability space, state and control.** Let $(\Omega_{\text{prob}}, \mathcal{F}, \{\mathcal{F}_t\}_{t\geq 0}, \mathbb{P})$ be a complete filtered probability space satisfying the usual conditions, supporting an N-dimensional standard Brownian motion $W = (W_t)_{t\geq 0}$. Here Ω_{prob} denotes the sample space (not to be confused with the spatial domain $\Omega \subset \mathbb{R}^N$).

Definition 4.1 (Admissible controls)**.** An admissible control is a progressively measurable process $v = (v_t)_{t\geq 0}$ with values in $\mathbb{R}^N$ such that

$$\mathbb{E}\left[\int_0^\tau |v_t|^\alpha \, dt\right] < \infty \quad \text{for all } x \in \Omega, \tag{4.2}$$

where τ is the exit time defined below. The set of admissible controls is denoted $\mathcal{U}_{\text{ad}}$.

For each $x \in \Omega$ and admissible control $v \in \mathcal{U}_{\text{ad}}$, the controlled state process $X^{x,v} = (X_t^{x,v})_{t\geq 0}$ is the unique strong solution to the stochastic differential equation

$$dX_t \;=\; v_t \, dt + \sigma \, dW_t, \qquad X_0 = x, \tag{4.3}$$

where $\sigma > 0$ is the diffusion coefficient. By standard SDE theory, (4.3) admits a unique strong solution continuous in t.

4.1.1. *Exit time and cost functional.*

Definition 4.2 (Exit time)**.** For each trajectory $X^{x,v}$, define the first exit time from the domain Ω by

$$\tau^{x,v} := \inf\{t > 0 : X_t^{x,v} \notin \Omega\}. \tag{4.4}$$

Since Ω is bounded and the diffusion is non-degenerate, we have $\mathbb{P}(\tau^{x,v} < \infty) = 1$ for all $x \in \Omega$.

Definition 4.3 (Cost functional)**.** Fix a running cost $h : \overline{\Omega} \to [0, \infty)$ that is continuous and sub-quadratic, and a constant boundary cost $g \in [0, \infty)$. For each $x \in \Omega$ and admissible control $v \in \mathcal{U}_{\text{ad}}$, define the cost functional

$$J(x; v) \;:=\; \mathbb{E}\left[\int_0^{\tau^{x,v}} \left(h(X_t^{x,v}) + |v_t|^\alpha\right) dt + g\right]. \tag{4.5}$$

The terminal cost g represents the cost incurred upon exiting the domain.

Definition 4.4 (Value function)**.** The value function is defined as

$$V(x) \;:=\; \inf_{v \in \mathcal{U}_{\text{ad}}} J(x; v), \quad x \in \Omega. \tag{4.6}$$

Under the sub-quadratic growth of h and boundedness of Ω, the cost functional $J(x; v)$ is finite for all admissible controls, ensuring that $V(x) < \infty$ for all $x \in \Omega$.

4.1.2. *Dynamic programming and verification.* We derive the HJB equation using the dynamic programming principle and Itô's formula. The approach proceeds in two stages: (i) a formal derivation via the martingale characterization, and (ii) a verification theorem confirming that smooth solutions to the HJB equation coincide with the value function.

Step 1: Martingale characterization. For a candidate value function $V \in C^2(\Omega) \cap C(\overline{\Omega})$, define the process

$$M_t := V(X_t^{x,v}) + \int_0^t \left(|v_s|^\alpha + h(X_s^{x,v})\right) ds, \quad t \in [0, \tau^{x,v}]. \tag{4.7}$$

The dynamic programming principle suggests that if V is the value function, then:

- M_t is a *supermartingale* for any admissible control v,
- M_t is a *martingale* for the optimal control v^*.

This characterization leads directly to the HJB equation.

Step 2: Applying Itô's formula. Applying Itô's formula to $V(X_t^{x,v})$ with X satisfying (4.3), we compute

$$\begin{aligned} dV(X_t^{x,v}) &= \nabla V(X_t^{x,v}) \cdot dX_t + \tfrac{1}{2} \operatorname{tr}\big(D^2 V(X_t^{x,v})\, d\langle X\rangle_t\big) \\ &= \nabla V(X_t^{x,v}) \cdot (v_t\, dt + \sigma\, dW_t) + \tfrac{1}{2} \operatorname{tr}\big(D^2 V(X_t^{x,v}) \cdot \sigma^2 I_N\big)\, dt \\ &= \nabla V(X_t^{x,v}) \cdot v_t\, dt + \tfrac{\sigma^2}{2} \Delta V(X_t^{x,v})\, dt + \sigma \nabla V(X_t^{x,v}) \cdot dW_t, \end{aligned} \tag{4.8}$$

where $\langle X\rangle_t = \sigma^2 t I_N$ is the quadratic variation matrix and $\Delta V = \operatorname{tr}(D^2 V)$ is the Laplacian.

Step 3: Differential of M_t. From (4.7) and (4.8),

$$dM_t = dV(X_t^{x,v}) + \big(|v_t|^\alpha + h(X_t^{x,v})\big)\, dt. \tag{4.9}$$

Substituting (4.8) into (4.9) yields

$$\begin{aligned} dM_t &= \nabla V(X_t^{x,v}) \cdot v_t\, dt + \tfrac{\sigma^2}{2} \Delta V(X_t^{x,v})\, dt + \sigma \nabla V(X_t^{x,v}) \cdot dW_t \\ &\quad + |v_t|^\alpha\, dt + h(X_t^{x,v})\, dt \\ &= \Big(\nabla V(X_t^{x,v}) \cdot v_t + \tfrac{\sigma^2}{2} \Delta V(X_t^{x,v}) + |v_t|^\alpha + h(X_t^{x,v})\Big)\, dt \\ &\quad + \sigma \nabla V(X_t^{x,v}) \cdot dW_t. \end{aligned} \tag{4.10}$$

Step 4: Drift condition and HJB inequality. For M_t to be a supermartingale, the drift term in (4.10) must be non-positive:

$$\nabla V(x) \cdot v + \tfrac{\sigma^2}{2} \Delta V(x) + |v|^\alpha + h(x) \le 0 \quad \text{for all } v \in \mathbb{R}^N, \quad x \in \Omega. \tag{4.11}$$

Rearranging (4.11),

$$-\tfrac{\sigma^2}{2} \Delta V(x) - h(x) \ge \nabla V(x) \cdot v + |v|^\alpha \quad \text{for all } v \in \mathbb{R}^N. \tag{4.12}$$

Step 5: HJB equation via optimization. Taking the infimum over all $v \in \mathbb{R}^N$ in (4.12), we obtain

$$-\tfrac{\sigma^2}{2} \Delta V(x) - h(x) \ge \inf_{v \in \mathbb{R}^N} \big\{\nabla V(x) \cdot v + |v|^\alpha\big\}. \tag{4.13}$$

For M_t to be a martingale under the optimal control (which characterizes the value function), equality must hold:

$$-\tfrac{\sigma^2}{2} \Delta V(x) - h(x) = \inf_{v \in \mathbb{R}^N} \big\{\nabla V(x) \cdot v + |v|^\alpha\big\}. \tag{4.14}$$

This is the Hamilton–Jacobi–Bellman equation in Hamiltonian form.

Step 6: Optimal control characterization. To solve the minimization problem in (4.14), we compute the first-order condition for the minimizer $v^*(x)$:

$$\nabla_v \left[\nabla V(x) \cdot v + |v|^\alpha\right] = 0, \tag{4.15}$$

which gives

$$\nabla V(x) + \alpha |v^*|^{\alpha-2} v^* = 0. \tag{4.16}$$

Solving (4.16) for v^* yields

$$v^*(x) = -\frac{1}{\alpha^{1/(\alpha-1)}} |\nabla V(x)|^{1/(\alpha-1)} \frac{\nabla V(x)}{|\nabla V(x)|} = -\frac{1}{\alpha^{1/(\alpha-1)}} |\nabla V(x)|^{\alpha-2} \nabla V(x). \tag{4.17}$$

This is the *feedback control law* in terms of the value function.

Step 7: Verification theorem.

Theorem 4.5 (Verification)**.** *Let $V \in C^2(\Omega) \cap C(\overline{\Omega})$ solve the HJB equation (4.14) with constant boundary condition $V = g$ on $\partial\Omega$, and assume that V satisfies polynomial growth. Define the feedback control $v^*(x)$ by (4.17). Then $V(x) = J(x; v^*)$ is the value function, and v^* is optimal.*

Proof. Let v be any admissible control. Applying Itô's formula to $V(X_t^{x,v})$ and using the HJB equation (4.14), we have:

$$\begin{aligned} \mathbb{E}[V(X_{T\wedge\tau}^{x,v})] &= V(x) + \mathbb{E}\left[\int_0^{T\wedge\tau} \left(\nabla V \cdot v + \tfrac{\sigma^2}{2}\Delta V\right) dt\right] \\ &\geq V(x) - \mathbb{E}\left[\int_0^{T\wedge\tau} \left(|v_t|^\alpha + h(X_t^{x,v})\right) dt\right]. \end{aligned}$$

The inequality follows from (4.11). Rearranging and letting $T \to \infty$, the bounded convergence theorem (since V is bounded on $\overline{\Omega}$ and has polynomial growth) and monotone convergence theorem for the integral yield $V(x) \leq J(x; v)$. Now, let v^* be the control defined by (4.17). For this control, equality holds in (4.11), so:

$$V(x) = \mathbb{E}\left[\int_0^\tau \left(|v_t^*|^\alpha + h(X_t^{x,v^*})\right) dt + V(X_\tau^{x,v^*})\right].$$

Since $V(X_\tau) = g$ on $\partial\Omega$, we obtain $V(x) = J(x; v^*)$, confirming that V is the value function and v^* is the optimal control. □

4.1.3. *Legendre transform yielding the quasilinear elliptic PDE.* We now compute the infimum in (4.14) explicitly using the Legendre–Fenchel transform.

Proposition 4.6 (Legendre transform)**.** *For $\xi \in \mathbb{R}^N$ and $\alpha \in (1, 2]$, we have*

$$\inf_{v \in \mathbb{R}^N} \left\{\xi \cdot v + |v|^\alpha\right\} = -\frac{\alpha - 1}{\alpha} |\xi|^{\frac{\alpha}{\alpha-1}} = -C_\alpha^{-1} |\xi|^p, \tag{4.18}$$

where $p = \alpha/(\alpha - 1) \in [2, \infty)$ and $C_\alpha = (\alpha - 1)/\alpha^p$.

Proof. The function $f(v) := \xi \cdot v + |v|^\alpha$ is strictly convex and coercive. The minimizer v^* satisfies the first-order condition

$$\xi + \alpha |v^*|^{\alpha-2} v^* = 0,$$

which gives

$$v^* = -\frac{1}{\alpha^{1/(\alpha-1)}}|\xi|^{1/(\alpha-1)}\frac{\xi}{|\xi|}.$$

Substituting back:

$$\begin{aligned} f(v^*) &= \xi\cdot\Big(-\frac{1}{\alpha^{1/(\alpha-1)}}|\xi|^{1/(\alpha-1)}\frac{\xi}{|\xi|}\Big) + \Big|\frac{1}{\alpha^{1/(\alpha-1)}}|\xi|^{1/(\alpha-1)}\frac{\xi}{|\xi|}\Big|^{\alpha} \\ &= -\frac{1}{\alpha^{1/(\alpha-1)}}|\xi|^{\alpha/(\alpha-1)} + \frac{1}{\alpha^{\alpha/(\alpha-1)}}|\xi|^{\alpha/(\alpha-1)} \\ &= |\xi|^{\alpha/(\alpha-1)}\Big(-\frac{1}{\alpha^{1/(\alpha-1)}} + \frac{1}{\alpha^{\alpha/(\alpha-1)}}\Big) \\ &= |\xi|^{p}\Big(-\frac{\alpha}{\alpha} + \frac{1}{\alpha^{p}}\Big)\cdot\frac{1}{\alpha^{1/(\alpha-1)}} = -\frac{\alpha-1}{\alpha^{p}}|\xi|^{p} = -C_{\alpha}^{-1}|\xi|^{p}. \end{aligned}$$

□

Applying Proposition 4.6 with $\xi = \nabla V(x)$ in (4.14), we obtain

$$-\tfrac{\sigma^2}{2}\Delta V(x) + \frac{\alpha-1}{\alpha^{p}}\,|\nabla V(x)|^{p} - h(x) = 0, \qquad x\in\Omega. \tag{4.19}$$

Multiplying through by -1 and recognizing $C_{\alpha}^{-1} = (\alpha-1)/\alpha^{p}$, we arrive at

$$-\frac{\sigma^2}{2}\Delta V(x) \;+\; C_{\alpha}\,|\nabla V(x)|^{p} - h(x) = 0, \quad x\in\Omega, \qquad V = g \text{ on } \partial\Omega. \tag{4.20}$$

This is precisely equation (1.1), the quasilinear Hamilton–Jacobi–Bellman equation studied by Lasry and Lions [10], for which we have established existence and uniqueness in Theorem 1.1.

5. Numerical Analysis

This section details the numerical implementation of the quasilinear HJB framework and its applications in operational research and imaging. The constructive nature of Theorem 1.1 makes it particularly suitable for numerical implementation. The monotone iteration scheme provides an algorithmic approach that is both theoretically sound and computationally efficient.

5.1. Weighted linear monotone iteration and stochastic simulation.

For the numerical approximation of the solution to the Hamilton–Jacobi–Bellman equation, we employ the *weighted monotone iteration* introduced by Lasry and Lions. This method is fully consistent with the analytical existence proof and is particularly robust on bounded domains. In addition, once the value function is computed, we construct the optimal feedback control and simulate the associated controlled diffusion.

The scheme constructs a decreasing sequence of functions $\{V^{(k)}\}_{k\geq 0}$ trapped between the ordered sub- and super-solutions

$$V_{-}(x) = g, \qquad V_{+}(x) = g + B\phi(x),$$

where ϕ is the torsion function solving $-\Delta\phi = 1$ in Ω, $\phi = 0$ on $\partial\Omega$, and $B \geq 2H/\sigma^2$ with $H = \max_{\overline{\Omega}} h$.

(1) **Preprocessing (torsion function and barriers).** Compute the torsion function ϕ solving

$$-\Delta\phi = 1 \quad \text{in } \Omega, \qquad \phi = 0 \quad \text{on } \partial\Omega.$$

Define the ordered barriers

$$V_-(x) := g, \qquad V_+(x) := g + B\phi(x), \quad B \geq \frac{2H}{\sigma^2}, \quad H := \max_{\overline{\Omega}} h.$$

(2) **Initialization.** Set the initial iterate

$$V^{(0)} := V_+ = g + B\phi.$$

(3) **Weighted linear monotone iteration.** For $k = 0, 1, 2, \ldots$ compute $V^{(k+1)}$ as the solution of

$$-\frac{\sigma^2}{2}\Delta V^{(k+1)} + \Lambda_0 V^{(k+1)} = h(x) + \Lambda_0 V^{(k)} - C_\alpha \big|\nabla V^{(k)}\big|^p \quad \text{in } \Omega, \tag{5.1}$$

with Dirichlet boundary condition

$$V^{(k+1)} = g \quad \text{on } \partial\Omega.$$

The constant weight $\Lambda_0 > 0$ is chosen so that the nonlinear Hamiltonian is dominated by the linear term:

$$\Lambda_0 \;\geq\; C_\alpha\, p\, M^{p-1}\, C_\Omega, \qquad M := \max\big\{\|\nabla V_-\|_{L^\infty}, \|\nabla V_+\|_{L^\infty}\big\},$$

where C_Ω is a Poincaré-type constant for the domain.

(4) **Monotonicity and projection.** After each linear solve, enforce the bounds

$$V_- \;\leq\; V^{(k+1)} \;\leq\; V_+ \quad \text{in } \Omega,$$

by projecting pointwise onto the interval $[V_-, V_+]$. This guarantees that the sequence remains ordered and uniformly bounded.

(5) **Convergence criterion.** Terminate the iteration when

$$\|V^{(k+1)} - V^{(k)}\|_{L^\infty(\Omega)} < \varepsilon,$$

for a prescribed tolerance $\varepsilon > 0$. The resulting limit $V := \lim_{k\to\infty} V^{(k)}$ is the numerical approximation of the value function.

(6) **Optimal feedback control.** Once V is computed, approximate its gradient ∇V on the grid and define the optimal feedback control $v^* = (v_1^*, v_2^*)$ by

$$v^*(x) = -\frac{1}{\alpha^{p-1}}\big|\nabla V(x)\big|^{p-2}\nabla V(x), \qquad p = \frac{\alpha}{\alpha - 1},$$

with the convention $v^*(x) = 0$ whenever $\nabla V(x) = 0$ or $x \notin \Omega$.

(7) **Stochastic dynamics simulation.** To illustrate the controlled dynamics, we simulate sample paths of the controlled diffusion

$$dX_t = v^*(X_t)\, dt + \sigma\, dW_t,$$

starting from an initial state $X_0 = x_0 \in \Omega$. On a time grid $t_n = n\Delta t$, $n = 0, \ldots, N$, we use the Euler–Maruyama scheme

$$X_{n+1} = X_n + v^*(X_n)\, \Delta t + \sigma\sqrt{\Delta t}\, \xi_n,$$

where $(\xi_n)_{n\geq 0}$ are independent standard Gaussian vectors in $\mathbb{R}^2$. The simulation is stopped when X_n approaches the boundary of Ω

(e.g., when the distance to $\partial\Omega$ falls below a prescribed margin), and the resulting trajectory is used to visualize the inventory dynamics under the optimal policy.

The operator on the left-hand side of (5.1) is coercive and order-preserving, and the right-hand side is monotone in $V^{(k)}$. Therefore the sequence $\{V^{(k)}\}$ is decreasing and converges to the unique classical solution of the HJB equation. This scheme is stable, monotone, and preserves the concavity of the value function in the quadratic case $\alpha = 2$ discovered in [2], while the stochastic simulation step provides a natural Monte Carlo illustration of the optimal controlled dynamics.

5.2. **Software implementation (radially symmetric case).** For the special case of radially symmetric problems ($\Omega = B_R(0)$ and h radial), numerical codes implementing the above algorithm are available in our companion repository [4].

5.3. **Applications to Production Planning and Image Enhancement.** The quasilinear HJB equation (1.1) arises in several applications:

- **Production planning:** The value function $V(x)$ represents the optimal production cost starting from inventory level x, with running cost $h(x)$ and control cost $|v|^\alpha$ representing production effort [2, 3].
- **Image restoration:** The parameter α controls the contrast enhancement in variational image processing models, with the HJB equation arising as the Euler-Lagrange equation [4].
- **Portfolio optimization:** In financial mathematics, V represents the value function of a portfolio optimization problem with transaction costs modeled by $|v|^\alpha$ [10].

We present a comprehensive numerical validation of the monotone iteration scheme. The implementation, developed in Python using high-precision sparse solvers, demonstrates the versatility of the quasilinear HJB framework in both operational research and computer vision. The codes solve the 2D quasilinear HJB PDE (1.1) directly on high-resolution grids (e.g., 241×241) using finite difference methods with efficient sparse solvers. This robust framework handles both the radial benchmark cases (1.2) and general non-radial domains, as extensively documented in [4, 3].

5.3.1. *Stochastic Production Planning Dynamics.* We evaluate the optimal production policy for a system governed by $\alpha = 1.5$ (leading to a cubic gradient penalty $p = 3$) on an elliptical inventory domain Ω. With parameters $\sigma = 0.3$ and boundary cost $g = 0.5$, the **Policy Iteration** solver converges rapidly to a tolerance of 10^{-6} in approximately 9 iterations. As illustrated in Figure 1, the value function $V(y)$ is strictly positive and concave, characterizing the minimal expected cost associated with varying inventory levels. The values range from 0.5 at the boundary to a peak of approximately 1.67 at the center, establishing a stable feedback production rate that drives the inventory toward the optimal set-point.

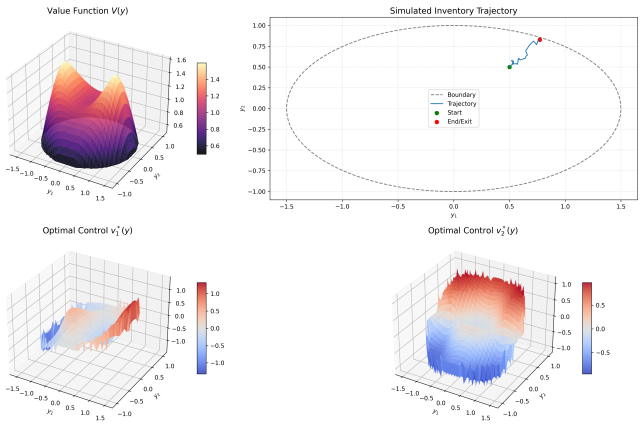

FIGURE 1. Numerical results for the stochastic production planning problem with $\alpha = 1.5$ and $h(y) = |y|^p$. Left: Value function $V(y)$. Center/Right: Optimal control components and simulated inventory trajectory.

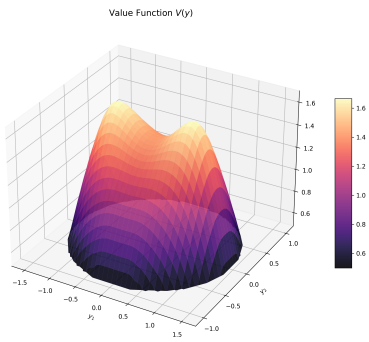

FIGURE 2. Numerical approximation of the value function $V(y)$ on the elliptical domain $\Omega = \{y : (y_1/1.5)^2 + y_2^2 < 1\}$ for $\alpha = 1.5$, $h(y) = |y|^p$, $\sigma = 0.3$, and boundary data $g = 0.5$. The surface rises monotonically from $V = 0.5$ on $\partial\Omega$ to a maximum of approximately 1.67 at the center, confirming the positivity result of Theorem 1.1. The Policy Iteration scheme converges in 9 steps to a tolerance of 10^{-6}.

Our Python code implementing the monotone iteration scheme used in the proofs of our results for the general quasilinear HJB elliptic equation on bounded domains, and which was used to generate the plots in this paper, can be found in [8].

5.3.2. *Contrast Enhancement via Nonlinear Hamilton–Jacobi–Bellman Dynamics.* Contrast enhancement is a fundamental operation in image processing, with direct impact on visual perception, feature extraction, and

downstream computer vision tasks. Classical approaches such as histogram equalization or total variation (TV) filtering operate either through global redistribution of intensities or local smoothing mechanisms. While effective in specific scenarios, these methods lack a principled mechanism for controlling the enhancement strength in relation to the underlying image geometry.

We propose a nonlinear contrast enhancement framework derived from the stationary Hamilton–Jacobi–Bellman (HJB) equation

$$-\frac{\sigma^2}{2}\Delta V(y) + C_\alpha \left|\nabla V(y)\right|^p - h(y) = 0, \qquad p = \frac{\alpha}{\alpha - 1},$$

where V is the value function defined on the chromaticity plane, $h(y)$ is a user-defined potential, and $\alpha > 1$ is the key parameter controlling the nonlinearity of the system. The enhanced image is obtained by advecting pixel values along the optimal drift field

$$b(y) = A_\alpha \left|\nabla V(y)\right|^{\frac{1}{\alpha-1}} \frac{\nabla V(y)}{|\nabla V(y)|}, \qquad A_\alpha = \left(\frac{1}{\alpha}\right)^{\frac{1}{\alpha-1}}.$$

Role of the Nonlinearity Parameter α. A central finding of our study is that the parameter α is the dominant factor governing the strength of contrast enhancement. When α approaches 1^+, the exponent $p = \alpha/(\alpha - 1)$ becomes large, amplifying the nonlinear gradient term and producing strong geometric enhancement. Conversely, larger values of α reduce the nonlinearity, yielding milder transformations.

This behavior is consistent with the theoretical structure of HJB equations: the term $|\nabla V|^p$ acts as a geometric amplifier of local intensity variations, and α directly modulates the sensitivity of the system to these variations. In contrast, the potential $h(y)$ influences only the forcing term and has a secondary effect on the global contrast dynamics.

Experimental Evaluation. We evaluate the proposed method on a representative RGB image and compare it against classical histogram equalization and a post-processed HJB+TV variant. Contrast quality is assessed using three widely adopted metrics: the Enhancement Measure Estimation (EME), the Tenengrad sharpness index, and the standard deviation of luminance.

Table 1 summarizes the results for a sweep of α values in the interval $[1.02, 2.0]$.

TABLE 1. Contrast metrics for various values of α. The proposed HJB method achieves its strongest enhancement for $\alpha \in [1.02, 1.10]$, significantly outperforming classical methods.

Method	EME	Tenengrad	StdDev
Original	5.59	106.63	70.91
Histogram Equalization	4.07	49.12	84.39
HJB ($\alpha = 1.02$–1.10)	7.97	187.16	85.53
HJB+TV ($\alpha = 1.02$–1.10)	10.06	148.72	85.28
HJB ($\alpha = 1.15$)	9.28	153.42	79.87
HJB+TV ($\alpha = 1.15$)	7.05	117.52	79.62
HJB ($\alpha = 1.20$)	6.84	123.08	74.19
HJB+TV ($\alpha = 1.20$)	4.86	90.57	73.97
HJB ($\alpha = 1.30$)	6.01	112.05	72.13
HJB+TV ($\alpha = 1.30$)	4.30	81.86	71.93
HJB ($\alpha = 1.50$)	5.81	109.15	71.53
HJB+TV ($\alpha = 1.50$)	4.18	79.62	71.33
HJB ($\alpha = 2.0$)	5.72	107.67	71.30
HJB+TV ($\alpha = 2.0$)	4.12	78.47	71.10

The results reveal a clear and consistent pattern:

- For $\alpha \in [1.02, 1.10]$, the HJB method produces the strongest enhancement, achieving EME = 7.97 and Tenengrad = 187.16, while the HJB+TV variant reaches EME = 10.06. This represents a substantial improvement over histogram equalization.
- The enhancement strength decreases gradually as α increases. The parameter α acts as a global contrast-control knob: small values produce aggressive sharpening, while larger values yield smoother, more conservative enhancement.
- For $\alpha \geq 1.3$, the method behaves similarly to a mild diffusion process, producing results close to the original image but still improving edge sharpness moderately.

FIGURE 3. Comparison between the original image, histogram equalization, the proposed HJB 2D PDE method ($\alpha = 1.15$), with $h(y) = |y|^p$, and the HJB 2D + TV variant. The composite figure illustrates the strong contrast enhancement achieved by the HJB approach, which significantly outperforms classical methods both visually and quantitatively.

Discussion. These findings demonstrate that the proposed HJB-based framework provides a mathematically rigorous and highly tunable mechanism for contrast enhancement. Unlike classical methods that lack a principled control parameter, the HJB formulation offers a single scalar α that continuously interpolates between strong geometric enhancement and gentle diffusive smoothing. This versatility, combined with superior performance in high-contrast regimes, establishes the HJB approach as a significant contribution to the field of variational image processing.

6. Conclusions and Future Directions

We have established the existence and uniqueness of classical solutions to the quasilinear Hamilton–Jacobi–Bellman equation (1.1) on bounded smooth convex domains under sub-quadratic growth conditions on the source term. The proof is constructive and provides a monotone iteration scheme that is amenable to numerical implementation. We have also derived the PDE from stochastic optimal control theory via the dynamic programming principle and verified that solutions to the PDE coincide with the value function of the associated control problem.

Several directions for future research include: (i) extension to degenerate diffusions where σ may vanish in parts of the domain, (ii) analysis of the singular limit $\alpha \to 1^+$ corresponding to $p \to \infty$, (iii) investigation of non-convex domains and the role of domain geometry, and (iv) higher-order regularity estimates beyond C^2.

Funding

This research received no external funding.

Data Availability Statement

No new data were created or analyzed in this study.

Conflicts of Interest

The author declares no conflict of interest.

Acknowledgments

The author thanks the anonymous referees for their careful reading and helpful suggestions that improved the presentation of this paper.

References

[1] Barles, G.; Perthame, B. Exit time problems in optimal control and vanishing viscosity method. *SIAM J. Control Optim.* **1988**, *26*, 1133–1148.

[2] Canepa, E.C.; Covei, D.-P.; Pirvu, T.A. A stochastic production planning problem. *Fixed Point Theory* **2022**, *23*, 179–198.

[3] Covei, D.-P. Stochastic production planning in manufacturing systems. *Axioms* **2025**, *14*(10), 766. https://doi.org/10.3390/axioms14100766

[4] Covei, D.-P. Image restoration via the integration of optimal control techniques and the Hamilton–Jacobi–Bellman equation. *Mathematics* **2025**, *13*(19), 3137. https://doi.org/10.3390/math13193137

[5] Crandall, M.G.; Ishii, H.; Lions, P.-L. User's guide to viscosity solutions of second order partial differential equations. *Bull. Amer. Math. Soc.* **1992**, *27*, 1–67.

[6] Fleming, W.H.; Soner, H.M. *Controlled Markov Processes and Viscosity Solutions*, 2nd ed.; Springer: New York, NY, USA, 2006.

[7] Gilbarg, D.; Trudinger, N.S. *Elliptic Partial Differential Equations of Second Order*, 2nd ed.; Springer-Verlag: Berlin, Germany, 2001.

[8] Our GitHub project https://github.com/coveidragos/code_contrast_image/blob/main/hjb_article_implementation_iter_alt.py

[9] Our GitHub project https://github.com/coveidragos/code_contrast_image/blob/main/contrast_nonradial_metrici.py

[10] Lasry, J.-M.; Lions, P.-L. Nonlinear elliptic equations with singular boundary conditions and stochastic control with state constraints. *Math. Ann.* **1989**, *283*, 583–630. https://doi.org/10.1007/BF01442856

[11] Lions, P.-L. Optimal control of diffusion processes and Hamilton–Jacobi–Bellman equations. Part 1: The dynamic programming principle and applications. *Comm. Partial Differential Equations* **1983**, *8*, 1101–1174.

[12] Perona, P.; Malik, J. Scale-space and edge detection using anisotropic diffusion. *IEEE Trans. Pattern Anal. Mach. Intell.* **1990**, *12*, 629–639.

[13] Rudin, L.I.; Osher, S.; Fatemi, E. Nonlinear total variation based noise removal algorithms. *Phys. D Nonlinear Phenom.* **1992**, *60*, 259–268.

Department of Applied Mathematics, The Bucharest University of Economic Studies, Piata Romana, 1st district, Postal Code: 010374, Postal Office: 22, Romania

Email address: dragos.covei@csie.ase.ro